

Evaluation of the Accuracy of Standardized Uptake Values of ^{18}F -fluorodeoxyglucose in Lung Lesions Based on Phantom Studies

DOI: 10.17691/stm2021.13.3.02

Received February 24, 2021



M.S. Tlostanova, MD, PhD, Leading Researcher, Department of Radiation Diagnostics¹; Physician-Radiologist, Department of Radioisotope Positron Emission Tomography¹;
L.A. Chipiga, PhD, Researcher, Laboratory of Radiation Hygiene of Medical Facilities²; Researcher¹;
 Associate Professor, Department of Nuclear Medicine and Radiation Technologies³

¹A.M. Granov Russian Research Center for Radiology and Surgical Technologies, Ministry of Health of the Russian Federation, 70 Leningradskaya St., Saint Petersburg, Pesochniy pos., 197758, Russia;

²Saint Petersburg Research Institute of Radiation Hygiene named after Professor P.V. Ramzaev, 8 Mira St., Saint Petersburg, 197101, Russia;

³Almazov National Medical Research Centre, Ministry of Health of the Russian Federation, 2 Akkuratova St., Saint Petersburg, 197341, Russia

The aim of the study was to estimate the accuracy of standardized uptake values of ^{18}F -fluorodeoxyglucose (^{18}F -FDG) in lung lesions during positron emission tomography combined with computed tomography (PET/CT) imaging, based on phantom studies performed for different PET/CT scanners.

Materials and Methods. The analysis of the PET/CT with ^{18}F -FDG data was performed for 86 patients newly diagnosed with the lung lesions: malignant tumors (n=37), benign tumors and inflammatory diseases (n=49). The criteria for inclusion in the study were developed considering the recommendations of the Fleischner Society (2017). The characteristics of the lesions on CT met the following requirements: a round shape or close to it; total size of 8 to 30 mm; solid or subsolid structure (with the exception of lesion with ground-glass opacity); a solid part size of ≥ 8 mm. All the patients had no signs of pleurisy, lymphadenopathy, or cancer history. PET/CT imaging with ^{18}F -FDG was performed with three scanners: Discovery 690 (General Electric, USA), Biograph mCT 128 (Siemens, Germany), and Biograph mCT 40 (Siemens); the preparation of patients prior to the scan was standardized. To determine the reference accumulation of a radiopharmaceutical in the pathological lesion, four scans of a specialized NEMA IEC PET Body Phantom Set (USA) were performed for each scanner. For each unit, the recovery coefficients (RCs) of radioactivity, maximum and recovered (corrected) standardized uptake values (SUVs) were determined. Statistical relationship between the size of lesions, SUV_{max} and $\text{SUV}_{\text{correct}}$ was evaluated. Data processing was performed using MedCalc v. 19.2.0 software.

Results. During the phantom study, the underestimation of the radioactivity was determined in the spheres with the diameters of 10 and 13 mm, overestimation was observed in the sphere with the diameter of 28 mm. Both underestimation and overestimation of radioactivity were determined for the spheres with a diameter of 17 and 22 mm.

SUV_{max} differed from the reference values for 85 patients (98.8%). The underestimation of these values was found for 63 patients (73.2%) due to the partial volume effect. The greatest underestimation was observed for the patients with 8 mm diameter lesions. Depending on the scanner, the underestimation of the SUV_{max} in these patients reached up to 54–73%. For 9 patients (25%) with malignant tumors of 9–12 mm, the utility of RC made it possible to avoid false negative results. For the lesions with a diameter of 30 mm, an overestimation of SUV_{max} up to 22% was determined due to the negative influence of the reconstruction algorithms.

Conclusion. The use of RC eliminates the influence of the partial volume effect and reconstruction methods on the accuracy of estimating the SUV_{max} in lung lesions, which ensures reproducibility, increase in the information content of the method, as well as the comparability of the results of PET/CT with ^{18}F -FDG obtained on the different models of PET/CT units with different technological characteristics.

Key words: PET/CT; ^{18}F -FDG; lung lesions; standardized uptake values; recovery coefficients; partial volume effect; NEMA IEC PET Body Phantom Set.

How to cite: Tlostanova M.S., Chipiga L.A. Evaluation of the accuracy of standardized uptake values of ^{18}F -fluorodeoxyglucose in lung lesions based on phantom studies. *Sovremennye tehnologii v medicine* 2021; 13(3): 15, <https://doi.org/10.17691/stm2021.13.3.02>

This is an open access article under the CC BY 4.0 license (<https://creativecommons.org/licenses/by/4.0/>).

Corresponding author: Marina S. Tlostanova, e-mail: tlostanovamarina@gmail.com

Introduction

Positron emission tomography (PET) is based on obtaining information about the biodistribution of a radiopharmaceutical in the patient's body. The accuracy of the evaluation of the radiopharmaceutical accumulation depends on the features of the detecting system of the scanner, radionuclide used, scanning protocol, data reconstruction algorithm, size of a pathological lesion, reconstruction and processing methods, etc [1]. According to the studies [1–4], the use of some data reconstruction methods with the time-of-flight (ToF) technology and point spread function (PSF) leads to overestimation of the standardized uptake values (SUVs). At the same time, an underestimation of the SUV_{max} for small lesions is associated with the partial volume effect (PVE) [5, 6].

The PVE concept combines two related phenomena that negatively affect both the qualitative characteristics of the images and the semi-quantitative values obtained during positron emission tomography combined with computed tomography (PET/CT) [5–7]. The first phenomenon is associated with the existing limitations of the spatial resolution of the PET modality and, as a consequence, blurring of the boundaries of the studied object on a three-dimensional image. This is due to the radioactivity “spill-over” and “spill-in” effects or, in other words, signal displacement from the focus to the surrounding tissues. Since a part of the detected signal becomes visible in the image outside the actual source, the PET images show the sizes of small tumors to seem significantly larger than real size. The second phenomenon is due to the presence of a tissue fraction. It consists of summing and subsequent averaging of the intensity of the detected signal from the tumor focus and nearby tissues, which leads to an artificial underestimation of SUV_{max} . This entails the

underestimation of the biological aggressiveness of the tumor and, as a consequence, an increase in the number of false negative results.

In other countries, one of the ways to correct PVE is the use of the recovery coefficient (RC), which is determined by scanning a specialized phantom of the NEMA IEC PET Body Phantom Set (USA), recommended by the National Electrical Manufacturers Association (NEMA) [8–10]. This procedure is performed on the ongoing basis, as a part of quality assurance. In the Russian Federation, it is advisory [11]. Meanwhile, the widespread use of RC could improve the accuracy of the method, as well as reproducibility and comparability of the results obtained in medical facilities on PET/CT scanners of various manufacturers with different technical characteristics.

The aim of this study was to estimate the accuracy of the evaluation of the standardized uptake values of ^{18}F -fluorodeoxyglucose (^{18}F -FDG) in lung lesions when performing positron emission tomography combined with computed tomography (PET/CT), based on phantom studies performed for different PET/CT scanners.

Materials and Methods

Phantom studies. Preparation of a dedicated NEMA IEC PET Body Phantom Set for PET/CT scanning consisted of filling the main volume and spheres with a ^{18}F solution. The appearance of the phantom and its components is shown in Figure 1.

The phantom spheres with diameters of 10, 13, 17, 22, and 28 mm were used to simulate lung lesions, the main volume of the phantom used as analogue of anatomical structures adjacent to the focus. The ^{18}F activity concentration in the main volume of the phantom was lower than that in the spheres. The prepared

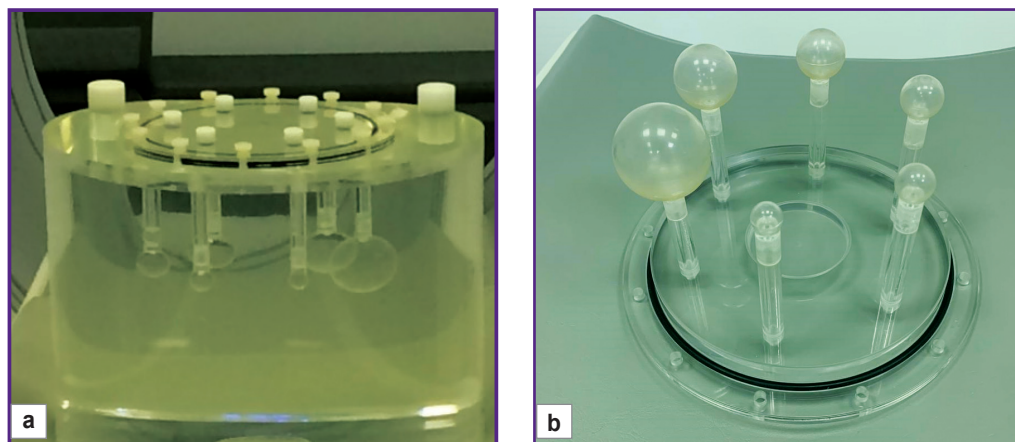


Figure 1. Appearance of the NEMA IEC PET Body Phantom Set (USA) and its components: (a) a main volume of the phantom with an inner length of 180 mm and a volume of 9.6 L; (b) six fillable spheres with inner diameters of 10, 13, 17, 22, 28, and 37 mm, the centers of which are located in the same plane; spheres' wall thickness — no more than 1 mm

Table 1
Radioactivity in the main volume of the phantom, spheres and the sphere–main volume ratio

Part of the phantom	Scans			
	1 st	2 nd	3 rd	4 th
Discovery 690				
Activity concentration (kBq/ml):				
total volume	0.36	0.43	0.76	1.2
spheres	3.7	3.0	2.5	2.1
Sphere–total volume activities ratio	10.3	7.0	3.3	1.7
Biograph mCT 128				
Activity concentration (kBq/ml):				
total volume	0.40	0.46	0.79	1.3
spheres	4.0	3.2	2.6	2.2
Sphere–main volume activities ratio	10.0	7.0	3.3	1.7
Biograph mCT 40				
Activity concentration (kBq/ml):				
total volume	0.34	0.40	0.72	1.1
spheres	3.3	2.8	2.4	1.9
Sphere–main volume activities ratio	9.7	7.0	3.3	1.7

phantom was scanned four times on each of the tested scanners: a Discovery 690 (General Electric, USA), a Biograph mCT 128 (Siemens, Germany), and a Biograph mCT 40 (Siemens) using the clinical protocols used for patients. Before each new scan, ¹⁸F was added to the total volume of the phantom to create a different ratio of the sphere–main volume. The analysis of the phantom images consisted of measuring radioactivity in the main volume of the phantom and in the spheres, as well as calculating the ratios of sphere–main volume. The radioactivity values in the main volume of the phantom, spheres, as well as the ratio of sphere–main volume for four scans, are presented in Table 1. The table shows that the radioactivity ratio in the spheres to the main volume at the 1st scan for the selected devices was 10.3; at the 2nd — 7.0; at the 3rd — 3.3; at the 4th — 1.7.

The parameters of the scan protocols and reconstruction, depending on the used PET/CT unit, are presented in Table 2.

The radioactivity of ¹⁸F was measured using a verified Curiementor 4 dose calibrator (PTW-Freiburg, Germany) with a relative 5% error in activity measuring. For each sphere, the volumes of interest were determined using automatic delineation in order to measure the maximum value of activity concentration. An example of delineation and measuring the maximum value of activity concentration in the spheres is shown in Figure 2.

To evaluate the reproduction of radioactivity in the

Table 2
Parameters of the scanning and reconstruction protocols for PET/CT scanners of different models

Parameter	Discovery 690	Biograph mCT 128	Biograph mCT 40
Scanning parameters			
Time per bed (min)	2.4	2.3	2.3
Scanning mode	WB	WB	WB
Bed overlapping	11	46	46
Reconstruction parameters			
Reconstruction method	VPFX + Sharp IR (ToF + PSF analogue)	ToF + PSF	ToF + PSF
Iteration/subset number	2/24	2/21	2/21
Reconstruction filter	Cut-Off 6.4	Hamm 5	Hamm 5
Image matrix (pixels)	192×192	256×256	256×256
Pixel size (mm)	3.64×3.64	3.18×3.18	3.18×3.18
Slice thickness (mm)	3.27	1.5	2.0

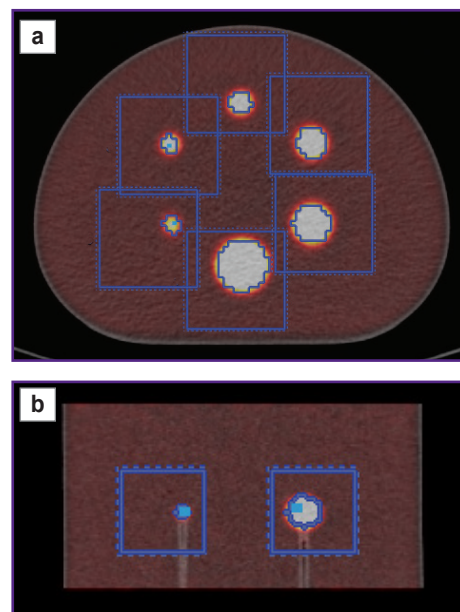


Figure 2. An example of delineating and measuring the maximum value of activity concentration in spheres in axial (a) and coronal (b) projections

lung lesions on the PET images, the RC was calculated by the formula

$$RC = \frac{A_{image}}{A_{inject}}$$

where A_{image} is the activity concentration in the sphere measured on PET images (kBq/ml); A_{inject} is the activity concentration injected into the sphere measured during preparation of the phantom for scanning (kBq/ml).

The RC values obtained for the four scans were averaged. The averaged RCs were interpolated for the unknown (intermediate) sizes of the lung lesions.

Patient studies. The analysis of the PET/CT with ¹⁸F-FDG data was carried out in 86 patients with solitary newly diagnosed lung lesions: in 37 patients with malignant tumors (MT), in 49 patients with benign tumors (BT) and inflammatory diseases (ID). The study was performed in accordance with the Declaration of Helsinki (2013) and approved by the Ethics Committee of the A.M. Granov Russian Research Center for Radiology and Surgical Technologies of the Ministry of Health of the Russian Federation.

The criteria for inclusion in the study were formed on the basis of the recommendations by the Fleischner Society [12]. The following characteristics of the lung lesions at CT were required: a round shape or close to it; total size — 8–30 mm; solid or subsolid structure (with the exception of the lesions with ground-glass opacity); solid part size ≥8 mm. At the time of PET/CT scanning, all the patients had no signs of pleurisy, lymphadenopathy, and an oncological history.

PET/CT with ¹⁸F-FDG was performed at the A.M. Granov Russian Research Center for Radiology and Surgical Technologies in the Department of Positron Emission Tomography on the Discovery 690, Biograph mCT 128, and Biograph mCT 40. The distribution of the patients into groups depended on the morphological diagnosis and the scanners are presented in Table 3.

The 60.5% of patients were scanned on a Discovery 690 scanner, 12.8% on a Biograph mCT 128 scanner, and 26.7% on a Biograph mCT 40 scanner. The preparation of patients prior to the scan was standardized. The study was limited to scanning one anatomical region — the thoracic region — and started 70–90 min after intravenous administration of ¹⁸F-FDG with the activity of 110 MBq per unit of the patient's body surface area. The scan protocol consisted of a topogram, helical CT scan without contrast enhancement for attenuation correction, and PET scan.

The post-processing data analysis consisted of visual evaluation of CT, PET, and hybrid images, as well as performing a semi-quantitative analysis. The measurement of SUVs was performed by automatic

delineation of the volume of interest (VOI) in a specialized program on an AW 4.7 workstation (General Electric). The SUV_{max} normalized to lean (muscle) body mass (SUL) were considered to be diagnostically significant levels of radiopharmaceutical uptake in the lung lesions. SUV_{max} (SUL) calculation was performed by the software package automatically according to the formula

$$SUV_{max} (SUL) = \frac{A_{VOI}}{A_{inject}/LBM},$$

where A_{VOI} is the radioactivity in the volume of interest (MBq/ml); A_{inject} is the total injected activity to the patient, corrected for lean (muscle) body mass (MBq/kg); LBM — lean body mass.

The corrected maximum SUVs (SUV_{correct}) were calculated by the formula

$$SUV_{correct} = \frac{SUV_{max}}{RC},$$

where SUV_{max} is the maximum level of radiopharmaceutical uptake in the lung lesions, on the PET image; RC is the ratio of the activity concentration in the sphere of the phantom, to the activity concentration injected into the sphere during the preparation of the phantom for scanning.

Statistical data processing. The data analysis was performed applying the MedCalc v. 19.2.0 software. The distribution was checked for normality using the Kolmogorov–Smirnov test (corrected for the Lilliefors). Applying the methods of descriptive statistics, the median and 95% confidence interval (CI) were calculated. The statistical significance of the differences between the values was calculated using the Wilcoxon test. The critical level of statistical significance of the null statistical hypothesis was taken equal to 0.05. Spearman's correlation coefficient (ρ) was calculated to study the relationship between the variables. The qualitative characteristic of the relationship between the studied variables was assessed using the Chaddock scale (0.10–0.30 — a weak relationship; 0.31–0.50 — a moderate relationship; 0.51–0.70 — a noticeable relationship; 0.71–0.90 is a high relationship; 0.91–1.0 is a very high relationship). For visual data representation, the box and whiskers plots were used.

Table 3

Patient distribution depending on the morphological diagnosis and the scanners (abs. number/%)

Diagnosis	Discovery 690	Biograph mCT 128	Biograph mCT 40
Malignant tumors (n=37)	24/64.9	3/8.1	10/27.0
Benign tumors and inflammatory diseases (n=49)	28/57.1	8/16.3	13/26.6
Total (n=86)	52/60.5	11/12.8	23/26.7

Results

Phantom studies. The RCs, averaged for dilutions and interpolated for unknown (intermediate) lesion sizes in the lungs, for four scans of the NEMA IEC PET Body Phantom Set with different ¹⁸F solution on three scanners, are presented in Table 4. The table demonstrates that the RCs varied relative to the value of 1.0 on all the scanners with different sizes of lesion. The RCs <1.0 indicated the underestimation of the radiopharmaceutical accumulation levels; the RCs >1.0 showed their overestimation; the RCs=1 demonstrated

Table 4

RCs averaged by four scans and interpolated for unknown (intermediate) lung lesion sizes of the NEMA IEC PET Body Phantom Set

Diameter (mm)	Recovery coefficients		
	Biograph mCT 128	Biograph mCT 40	Discovery 690
30	1.22	1.20	1.05
29	1.20	1.19	1.04
28	1.19	1.18	1.03
27	1.16	1.17	1.02
26	1.14	1.16	1.0
25	1.12	1.15	0.99
24	1.09	1.14	0.98
23	1.07	1.13	0.97
22	1.04	1.12	0.95
21	1.02	1.10	0.92
20	0.99	1.08	0.89
19	0.97	1.06	0.86
18	0.94	1.04	0.83
17	0.92	1.02	0.80
16	0.89	0.98	0.77
15	0.86	0.94	0.73
14	0.83	0.90	0.70
13	0.80	0.87	0.66
12	0.72	0.77	0.57
11	0.64	0.67	0.48
10	0.56	0.58	0.39
9	0.49	0.48	0.30
8	0.46	0.38	0.27

accordance with the radiopharmaceutical accumulation levels with the reference values.

Patient studies. In 37 patients with MT, the sizes of the detected lung lesions on the CT images ranged from 8 to 30 mm (median — 16.5; 95% CI 13.0–18.0). A direct correlation between the lesion size and SUV_{max} was found ($p=0.59$; 95% CI 0.33–0.77; $p=0.0001$). No correlation was found between the size of the lesions and $SUV_{correct}$ ($p=0.24$; 95% CI 0.09–0.53; $p=0.1546$). The SUV_{max} and $SUV_{correct}$ are shown in Figure 3.

The values in the box plots show the minimum and maximum values, 25th and 75th percentiles, and medians with 95% CI. The outliers were considered to be the values lying in the ranges exceeding the height of the box from its upper and lower boundaries by 1.5 times.

Figure 3 shows that SUV_{max} in patients with MT had a wide range (from 0.6 to 27.5), differed among themselves significantly ($p<0.0001$); the median was determined at the level of 1.9 (95% CI 1.5–2.4). After applying

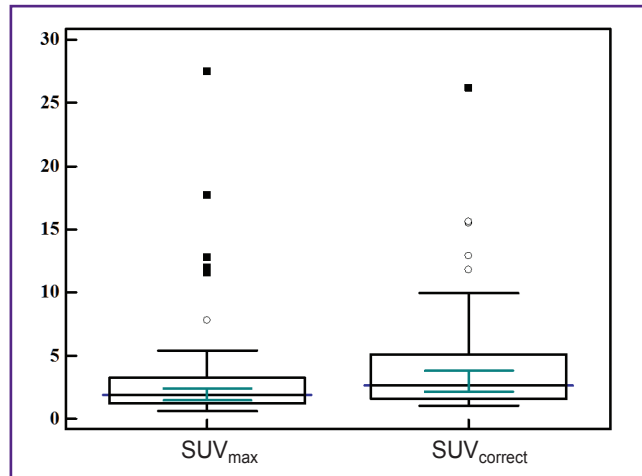


Figure 3. The range of SUV_{max} and $SUV_{correct}$ in the patients with malignant tumors in the lungs

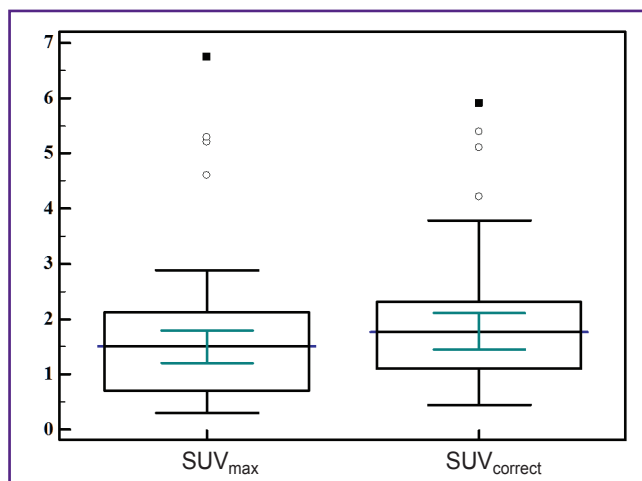


Figure 4. The range of SUV_{max} and $SUV_{correct}$ values in the patients with benign tumors and inflammatory lung disease

the RC, the corrected levels of radiopharmaceutical accumulation were determined within the range of 1.1–26.2, the median $SUV_{correct}$ was 2.6 (95% CI 2.1–3.8). No statistically significant differences were found ($p=0.0024$) between SUV_{max} and $SUV_{correct}$.

In 49 patients with BT and ID the size of the detected lesions on the CT images varied from 8 to 29 mm, the median was 16.0 (95% CI 14.0–18.8). When comparing the size of the lesion and the SUV_{max} , a direct high correlation was found between these characteristics ($p=0.61$; 95% CI 0.39–0.76; $p<0.0001$). No correlation was found between the lesion size and $SUV_{correct}$ ($p=0.19$; 95% CI 0.09–0.45; $p=0.1872$). The SUV_{max} and $SUV_{correct}$ recorded in the patients with BT and ID are shown in Figure 4.

The values in the box plots show the minimum and maximum values, 25th and 75th percentiles, and medians with 95% CI. The outlying values were considered those

Table 5
Distribution of the examined patients according to the RC

Diagnosis	RC <1.0			RC=1.0			RC >1.0		
	Number of patients (abs. number/%)	Lesion size (mm) [median (95% CI)]	SUV _{max} [median (95% CI)]	Number of patients (abs. number/%)	Lesion size (mm) [median (95% CI)]	SUV _{max} [median (95% CI)]	Number of patients (abs. number/%)	Lesion size (mm) [median (95% CI)]	SUV _{max} [median (95% CI)]
Malignant tumors (n=37)	28/75.7	14.2 (11–17)	1.5 (1.2–1.9)	1/2.7	26	11.6	8/21.6	23.5 (18.0–29.2)	6.3 (2.6–20.0)
Benign tumors and inflammatory diseases (n=49)	35/71.4	14.5 (12–15)	1.2 (0.7–1.5)	—	—	—	14/28.6	24 (21–26)	2.1 (1.5–3.1)
Total (n=86)	63/73.2	14.4 (13–15)	1.8 (1.1–1.5)	1/1.2	—	—	22/25.6	24 (21–26)	2.7 (1.9–5.2)

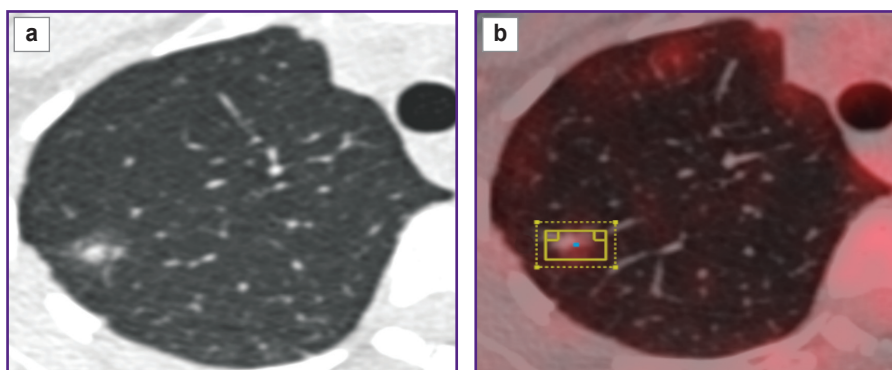


Figure 5. Diagnosis: “acinar adenocarcinoma of the upper lobe of the right lung; G2; pT1aN0cM0; IA”. The study was performed on a PET/CT Discovery 690: (a) CT scan in the S3 segment of the right lung detects a subsolid lesion with the total size 12 and 8 mm of the solid part; (b) PET detects a lesion that minimally accumulates radiopharmaceutical; SUV_{max}=0.9; RC=0.27; SUV_{correct}=3.5

690. According to the phantom studies, the RC on this scanner equals 1 when the focus size is 26 mm.

It is important to note the clinical significance of the obtained findings. A considerable underestimation of SUV_{max} nearly leads to obtaining false negative results in 9 MT patients (32.1%) with the lung lesions ranged from 9 to 12 mm. In all these cases, due to the low level of radiopharmaceutical uptake in the MT, the changes in the lung were erroneously interpreted as an inflammatory process. Applying RC in these patients ensured objective assessment

lying in the ranges exceeding the height of the box from its upper and lower boundaries by 1.5 times.

Figure 4 shows that the SUV_{max} in the patients with BT and ID were determined in the range of 0.3–6.7; the median was 1.5 (95% CI 1.2–1.8). After applying the RC, the corrected levels of radiopharmaceutical accumulation ranged from 0.5 to 5.9; the median was 1.8 (95% CI 1.5–2.1). The comparison of SUV_{max} and SUV_{correct} showed statistically significant differences (p=0.0006).

Table 5 shows the frequency distribution of the examined patients, depending on the RC value. The table shows that the overwhelming number of the patients, regardless of the morphological diagnosis, showed a distortion of the levels of radiopharmaceutical accumulation. Most often (73.2%), the underestimation of SUV_{max} was recorded in the lesions from 10 to 20 mm. The SUV_{max} overestimation was observed in 25.6% of the patients with larger lesions (20–28 mm). Only in one case, the measured level of radiopharmaceutical uptake in the tumor corresponded to the reference value in a patient with MT scanned on the PET/CT Discovery

of the radiopharmaceutical accumulation levels and, as a consequence, correctly suggested the nature of the tumor (Figure 5).

Thus, the results of the phantom and patient studies show that, regardless of the used scanners in the lesions up to 20 mm during PET/CT scanning, a considerable underestimation of SUV_{max} is observed. It might lead to underestimation of the biological aggressiveness of a tumor and, as a consequence, an increase in the number of false negative results. At the same time, with larger lesion sizes, depending on the scanner model, SUV_{max} overestimation may be observed. All these distortions in the value measurements in the routine practice of PET departments must undoubtedly be corrected.

Discussion

Currently, PET/CT is one of the principal methods of diagnostics and evaluation of the treatment effectiveness of various oncological diseases. The given technology is characterized by substantially high visualizing

capabilities and, at the same time, is a qualitative method that allows for measuring various biochemical processes ongoing in the human body. To solve clinical problems with the utility of PET/CT as quantitative criteria, different indicators are used: SUV_{max} , metabolic tumor volume (MTV), total lesion glycolysis (TLG), average ratio of the tumor-to-background radioactivity (TBR), standardized uptake peak value determined within the VOI of the fixed size (SUV_{peak}), etc. [13–18]. The most common one among them is SUV_{max} , which is determined by the semiquantitative method [15].

SUV displays the intensity of radiopharmaceutical accumulation in the target volume of interest and depends on the volume in which the given activity is spread [15]. There are several techniques of calculating SUVs depending on the patient's body mass, surface area of the body, as well as SUL [15, 19, 20]. In compliance with the latest recommendations by the European Association of Nuclear Medicine (EANM), the definition of SUL. At the same time, it is important to note that SUV_{max} , as well as other quantitative values, depends on several factors: a glucose level in the patient's blood plasma, duration of radiopharmaceutical accumulation, parameters of the scan protocol, data reconstruction algorithms, accuracy of volume of interest determination and delineation method, intensity of radiopharmaceutical accumulation in the adjoining tissues, heterogeneity of a lesion structure, etc [1–7].

Another important factor that affects both the qualitative and quantitative characteristics of PET images is PVE [5–7]. This effect is based on the existing limitations in the spatial resolution of PET modality, which lead to unsatisfactory visualization of small tumors and underestimation of SUV_{max} relative to the true levels of radiopharmaceutical accumulation. Because of PVE, the lesions with the same level of radiopharmaceutical accumulation, but differing size and histological origin, are displayed on PET images with different brightness. As a result, tumors of a malignant nature may be erroneously regarded as less aggressive, and this leads to an increase in the number of false negative results at PET/CT with ^{18}F -FDG.

Today, the most famous and easily reproducible method for PVE correction is the use of RC, which is determined on the basis of the phantom studies [15, 21]. According to the obtained data, the RC becomes close to 1.0 with the increase in lesion size. In other words, the small lesions are more affected the underestimation of radiopharmaceutical accumulation. Thus, the negative effect of PVE in the lesion with a diameter of 8 mm led to SUV_{max} underestimation from 54 to 73% for different scanners. At the same time, in 9 patients having MT with the size of the pathological lung lesions ranged from 9 to 12 mm, the use of RC avoids false negative results. In all these cases, the MT was not clearly visible on the background of an intact lung, and the SUV_{max} for the lesion did not exceed 1.0.

According to the literature [6, 15, 21], the impact

of PVE becomes more detectable for the lung lesions located near the anatomical structures, which are normally characterized by an increased radiopharmaceutical accumulation. Usually, at PET/CT with ^{18}F -FDG imaging, physiological radiopharmaceutical pathological accumulation is observed in the mediastinum, liver, left ventricular myocardium, and ribs. According to these studies, RC may be ineffective for the tumors located close to at least two anatomical structures with different radiopharmaceutical accumulation.

The severity of the PVE also depends on the shape of the tumor. It is generally assumed that PVE is more pronounced for larger the surface area of the pathological lesions [6, 22]. Accordingly, tumors that have a spherical, i.e., more compact form, are less susceptible to a negative impact of PVE. This is due to the fact that in the lesions of an irregular shape and/or heterogeneous structure the zone of necrotic softening is located in the center and volume with actively accumulates radiopharmaceutical is located mainly in the peripheral parts of the tumor. In these cases, intensive processes of radioactivity “spill-over” between the periphery of the tumor, adjoining anatomical structures and the necrotic center of the tumor, determine the strong influence of PVE on the quantitative PET characteristics.

On the other hand, the pathological lesions with the diameter of 30 mm showed a marked SUV_{max} overestimation — by 22%. According to the literature [1–3, 16, 23, 24], SUVs overestimation is connected with reconstruction algorithms, such as PSF and ToF. Both algorithms are used in modern hybrid scanners to increase the sensitivity of the PET/CT method, improving the signal/noise ratio and reducing the scan duration. As shown in the given study, the negative influence of the reconstruction methods on SUV_{max} in the lesion of a larger size can also be eliminated with the RC. Correction of SUVs in these cases can prevent obtaining false positive results.

Direct correlation between SUV_{max} and the sizes of the lung lesions was confirmed by the results of numerous studies [25–28]. In the course of the given study, the statistical correlation between these criteria was found in the patients of both groups. It should be noted that, after applying RC, the statistical correlation between the lesion sizes and $SUV_{correct}$ was not determined for all morphological diagnoses and scanners. It evidenced that RC eliminated a negative impact of PVE on SUV_{max} in the small lesions and also showed the influence of the reconstruction methods on the larger lesions.

In 2010, the EANM launched a accreditation programme (European Association Research Limited, EARL) of the medical facilities performing PET/CT with ^{18}F -FDG [2, 10, 23, 28–31]. This strategy was aimed at minimization of variability of qualitative PET-criteria by standardization of the data acquisition and reconstruction protocols. Currently, the EARL programme validation is described as the evaluation of the effectiveness of treatment of MT in various tissues including lung cancer.

By 2016, the Clinical Trials Network (CTN) collected in the accredited EANM–EARL system the results of 2500 phantom studies were obtained approximately in 200 scanners of different models in 150 medical facilities around the world [10].

Today, professional societies as the American College of Radiology Imaging Network (ACRIN), the Radiologic Society of North America's Quantitative Imaging Biomarker Alliance, American Association of Physicists in Medicine are also actively working to promote the concept of harmonization of PET/CT [30]. In our country, this area has just begun to develop. In 2020, Rospotrebnadzor published the methodological guidelines for optimization of the quality control procedures and stability of PET image parameters using the phantom [11].

Conclusion

The use of the recovery coefficient neutralizes the PVE and impact of the reconstruction methods on the accuracy of SUV_{max} in the lung lesions, which allows for increasing the information of the PET/CT with ^{18}F -FDG method and ensures the reproducibility and comparability of the results obtained on the scanners of different models with different technological characteristics.

Study funding. The study was not funded by any sources.

Conflicts of interest. No obvious or potential conflicts of interest relevant to the publication of this article were reported.

References

1. Westertep M., Pruim J., Oyen W., Hoekstra O., Paans A., Visser E., van Lanschot J., Sloof G., Boellaard R. Quantification of FDG PET studies using standardized uptake values in multi-center trials: effects of image reconstruction, resolution and ROI definition parameters. *Eur J Nucl Med Mol Imaging* 2007; 34(3): 392–404, <https://doi.org/10.1007/s00259-006-0224-1>.
2. Lasnon C., Hicks R.J., Beaugard J.M., Milner A., Paciencia M., Guizard A.V., Bardet S., Gervais R., Lemoel G., Zalman G., Aide N. Impact of point spread function reconstruction on thoracic lymph node staging with ^{18}F -FDG PET/CT in non-small cell lung cancer. *Clin Nucl Med* 2012; 37: 971–976, <https://doi.org/10.1097/rlu.0b013e318251e3d1>.
3. Armstrong I.S., Kelly M.D., Williams H.A., Matthews J.C. Impact of point spread function modelling and time of flight on FDG uptake measurements in lung lesions using alternative filtering strategies. *EJNMMI Phys* 2014; 1(1): 99, <https://doi.org/10.1186/s40658-014-0099-3>.
4. Lindström E., Sundin A., Trampal C., Lindsjö L., Ilan E., Danfors T., Antoni G., Sörensen J., Lubberink M. Evaluation of penalized-likelihood estimation reconstruction on a digital time-of-flight PET/CT scanner for ^{18}F -FDG whole-body examinations. *J Nucl Med* 2018; 59(7): 1152–1158, <https://doi.org/10.2967/jnumed.117.200790>.
5. Bettinardi V., Castiglioni I., De Bernardi E., Gilardi M.C. PET quantification: strategies for partial volume correction. *Clin Transl Imaging* 2014; 2: 199–218, <https://doi.org/10.1007/s40336-014-0066-y>.
6. Soret M., Bacharach S.L., Buvat I. Partial-volume effect in PET tumor imaging. *J Nucl Med* 2007; 8(6): 932–945, <https://doi.org/10.2967/jnumed.106.035774>.
7. Hofeinz F., Langner J., Petr J., Beuthien-Baumann B., Oehme L., Steinbach J., Kotzerke J., van den Hoff J. A method for model-free partial volume correction in oncological PET. *EJNMMI Res* 2012; 2(1): 16, <https://doi.org/10.1186/2191-219x-2-16>.
8. NEMA Standards Publication. NEMA NU2-2018. Performance measurement for Positron Emission Tomographs (PET). VA, USA: National Electrical Manufacturer Association; 2018.
9. Pasawang P., Sontrapornpol T., Krisanachinda A. Experience on performance measurements of positron emission tomographs: NEMA NU2-2018. *Med Phys Int* 2019; 7(3): 305–313.
10. Kaalep A., Sera T., Oyen W., Krause B.J., Chiti A., Liu Y., Boellaard R. EANM/EARL FDG-PET/CT accreditation — summary results from the first 200 accredited imaging systems. *Eur J Nucl Med Mol Imaging* 2018; 45(3): 412–422, <https://doi.org/10.1007/s00259-017-3853-7>.
11. Rospotrebnadzor. Metodicheskie ukazaniya MUK 2.6.7.3651-20 “Metody kontrolya v PET-dagnostike dlya optimizacii radiacionnoj zashchity” [Methodical guidelines MUK 2.6.7.3651-20 “Methods of control in PET diagnostics to optimize radiation protection”]. Moscow; 2020; p. 34.
12. MacMahon H., Naidich D., Goo J., Lee K.C., Leung A.N.C., Mayo J.R., Mehta A.C., Ohno Y., Powell C.A., Prokop M., Rubin G.D., Schaefer-Prokop C.M., Travis W.D., Van Schil P., Bankier A.A. Guidelines for management of incidental pulmonary nodules detected on CT images: from the Fleischner Society 2017. *Radiology* 2017; 84(1): 228–243, <https://doi.org/10.1148/radiol.2017161659>.
13. Mukhortova O.V., Aslanidi I.P., Ashrafyan L.A., Shurupova I.V., Derevyanko E.P., Katunina T.A., Alimardonov D.B., Ulyanova A.V. ^{18}F -fluorodeoxyglucose positron emission tomography in cancer patients: a whole-body examination procedure. *Opuholi zenskoj reproduktivnoj sistemy* 2009; 3–4: 70–77.
14. Yablonskiy P.K., Tlostanova M.S., Avetisyan A.O. Efficacy of PET with ^{18}F -FDG in differential diagnosis of lung cancer by calculation of standardized uptake value and tumor/lung criterion. *Vestnik Sankt-Peterburgskogo universiteta. Seriya 11. Medicina* 2012; 1: 157–164.
15. Boellaard R., Delgado-Bolton R., Oyen W.J.G., Giammarile F., Tatsch K., Eschner W., Verzijlbergen F.J., Barrington S.F., Pike L.C., Weber W.A., Stroobants S., Delbeke D., Donohoe K.J., Holbrook S., Graham M.M., Testanera G., Hoekstra O.S., Zijlstra J., Visser E., Hoekstra C.J., Pruim J., Willemsen A., Arends B., Kotzerke J., Bockisch A., Beyer T., Chiti A., Krause B.J.; European Association of Nuclear Medicine (EANM). FDG PET/CT: EANM procedure guidelines for tumour imaging: version 2.0. *Eur J Nucl Med Mol Imaging* 2015; 42(2): 328–354, <https://doi.org/10.1007/s00259-014-2961-x>.
16. Sher A., Lacoëuille F., Fosse P., Vervueren L., Cahouët-Vannier A., Dabli D., Bouchet F., Couturier O. For avid glucose tumors, the SUV peak is the most reliable parameter for [^{18}F] FDGPET/CT quantification, regardless of acquisition time.

EJNMMI Res 2016; 6(1): 21, <https://doi.org/10.1186/s13550-016-0177-8>.

17. Zhang Q., Gao X., Wei G., Qiu C., Qu H., Zhou X. Prognostic value of MTV, SUV_{max} and the T/N ratio of PET/CT in patients with glioma: a systematic review and meta-analysis. *J Cancer* 2019; 10(7): 1707–1716, <https://doi.org/10.7150/jca.28605>.

18. Li Q., Zhang J., Cheng W., Zhu C., Chen L., Xia F., Wang M., Yang F., Ma X. Prognostic value of maximum standard uptake value, metabolic tumor volume, and total lesion glycolysis of positron emission tomography/computed tomography in patients with nasopharyngeal carcinoma: a systematic review and meta-analysis. *Medicine* 2017; 96(37): e8084, <https://doi.org/10.1097/md.0000000000008084>.

19. Keyes J.W. Jr. SUV: standard uptake or silly useless value? *J Nucl Med* 1995; 36(10): 1836–1839.

20. Sugawara Y., Zasadny K.R., Neuhoff A.W., Wahl R.L. Reevaluation of the standardized uptake value for FDG: variations with body weight and methods for correction. *Radiology* 1999; 213(2): 521–525, <https://doi.org/10.1148/radiology.213.2.r99nv37521>.

21. Aide N., Lasnon C., Veit-Haibach P., Sera T., Sattler B., Boellaard R. EANM/EARL harmonization strategies in PET quantification: from daily practice to multicentre oncological studies. *Eur J Nucl Med Mol Imaging* 2017; 44 (Suppl 1): 17–31, <https://doi.org/10.1007/s00259-017-3740-2>.

22. Hoetjes N.J., van Velden F.H., Hoekstra O.S., Hoekstra C.J., Krak N.C., Lammertsma A.A., Boellaard R. Partial volume correction strategies for quantitative FDG PET in oncology. *Eur J Nucl Med Mol Imaging* 2010; 37: 1679–1687, <https://doi.org/10.1007/s00259-010-1472-7>.

23. Sonni I., Baratto L., Park S., Hatami N., Srinivas S., Davidzon G., Gambhir S.S., Iagaru A. Initial experience with a SiPM-based PET/CT scanner: influence of acquisition time on image quality. *EJNMMI Phys* 2018; 5(1): 9, <https://doi.org/10.1186/s40658-018-0207-x>.

24. Wagatsuma K., Miwa K., Sakata M., Oda K., Ono H.,

Kameyama M., Toyohara J., Ishii K. Comparison between new-generation SiPM-based and conventional PMT-based TOF-PET/CT. *Phys Med* 2017; 42: 203–210, <https://doi.org/10.1016/j.ejmp.2017.09.124>.

25. Granov A.M., Tyutin L.A., Tlostanova M.S., Avetisyan A.O., Ryzhkova D.V. Optimization of quantitative processing data of positron emission tomography with ¹⁸F-FDG in patients with lung cancer. *Sovremennye tehnologii v medicine* 2012; 1: 44–48.

26. Tlostanova M.S., Avetisyan A.O. The informativeness of positron emission tomography with [¹⁸F]-fluorodeoxyglucose in differential diagnosis of lung cancer. *Vestnik Rossiyskogo gosudarstvennogo meditsinskogo universiteta* 2012; 2: 41–44.

27. Khalaf M., Abdel-Nabi H., Baker J., Shao Y., Lamonica D., Gona J. Relation between nodule size and ¹⁸F-FDG-PET SUV for malignant and benign pulmonary nodules. *J Hematol Oncol* 2008; 1–8: 13, <https://doi.org/10.1186/1756-8722-1-13>.

28. Yilmaz F., Tastekin G. Sensitivity of ¹⁸F-FDG PET in evaluation of solitary pulmonary nodules. *Int J Clin Exp Med* 2015; 8(1): 45–51.

29. Christian P.E. Use of a precision fillable clinical simulator phantom for PET/CT scanner validation in multicenter clinical trials: the SNM Clinical Trials Network (CTN) Program. *J Nucl Med* 2012; 53(Suppl 1): 437.

30. Lasnon C., Quak E., Le Roux P.Y., Robin F., Hofman M.S., Bourhis D., Callahan J., Binns D.S., Desmots C., Salaun P.Y., Hicks R.J., Aide N. EORTC PET response criteria are more influenced by reconstruction inconsistencies than PERCIST but both benefit from the EARL harmonization program. *EJNMMI Physics* 2017; 4(1): 17, <https://doi.org/10.1186/s40658-017-0185-4>.

31. Sunderland J.J., Christian P.E. Quantitative PET/CT scanner performance characterization based upon the society of nuclear medicine and molecular imaging clinical trials network oncology clinical simulator phantom. *J Nucl Med* 2015; 56(1): 145–152, <https://doi.org/10.2967/jnumed.114.148056>.